

Increase in the signal-to-noise ratio of the beat note between a frequency comb and a continuous-wave laser

Shen Zhang^{1,2,3}, Qi Shen,^{1,2,3,*} Lei Hou,^{1,2,3} Jian-Yu Guan^{1,2,3}, Shengkai Liao^{1,2,3,†}, Qiang Zhang,^{1,2,3} and Hai-Feng Jiang^{1,2,3}

¹*Hefei National Research Center for Physical Sciences at the Microscale and School of Physical Sciences, University of Science and Technology of China, Hefei, 230026 Anhui, China*

²*Shanghai Research Center for Quantum Science and CAS Center for Excellence in Quantum Information and Quantum Physics, University of Science and Technology of China, 201315 Shanghai, China*

³*Hefei National Laboratory, University of Science and Technology of China, Hefei, 230088 Anhui, China*

(Received 23 October 2023; revised 2 March 2024; accepted 14 March 2024; published 29 March 2024)

For most comb-based applications, the signal-to-noise ratio (SNR) of the beat note between the comb and the continuous-wave laser is a critical parameter that affects the stability of the system and the accuracy of the measurement. We analyze the SNR model of the beat note and discuss some key aspects of implementing an optimized gated-detection scheme. High-speed balanced detection is introduced to enable detection of more interfering photons, while suppressing optical-intensity-noise interference. The gated detection is achieved by our combining a self-made low-noise, delay-adjustable pulse-generator circuit, which can suppress phase-random white noise. Compared with traditional direct-detection schemes, we demonstrate a 20-dB improvement in performance and achieve a beat-note SNR of more than 60 dB within a 300-kHz resolution bandwidth. Further experiments on frequency-comb locking show that this scheme has high reliability and robustness.

DOI: 10.1103/PhysRevApplied.21.034066

I. INTRODUCTION

Over the past 20 years, frequency combs have been widely used and developed in the field of precision measurement, such as optical frequency measurement [1], time-frequency transfer based on dual-comb spectroscopy [2,3], and atmospheric spectroscopy analysis [4]. These applications require the frequency comb to be referenced to a stable laser, which can be achieved by detecting the beat note between the frequency comb and the laser, and by using feedback control to adjust the length of the frequency-comb cavity [5,6]. The beat-note signal-to-noise ratio (SNR) of the frequency comb and the laser affects the reliability of the optical system and the accuracy of the measurement results. Increasing the SNR of the beat note helps to reduce the phase-slip phenomenon in frequency measurement [7], provide a greater measurement bandwidth, and improve the system's anti-interference capability with regard to external disturbances [8,9].

The SNR of the beat note between a frequency comb and a continuous-wave (cw) laser is typically constrained by two factors: the power of a single comb tooth and the noise in the detection process. Because of the large number

of comb teeth present in the frequency-comb spectrum, the tooth power effectively contributing to the heterodyne beat is limited [8]. This limitation will become more pronounced in future space-ground applications due to the degradation of Er-doped-fiber performance caused by radiation [10,11], making long-term stable operation of the frequency-comb system a challenge. The same problem arises when one is simultaneously detecting multiple optical beat signals in a single-branch comb, as it is difficult to optimize the available power for multiple regions of the comb spectrum [7,12]. In addition, detector noise performance and optical noise also constrain the increase of the SNR, especially the shot-noise part, which imposes a limit on the SNR. These noise components are typically considered to be uncorrelated, while there is a high degree of phase correlation between the teeth of the frequency comb. Leveraging this characteristic, Deschênes *et al.* [13] proposed a gated-detection scheme to increase the energy-utilization efficiency of the frequency comb and suppress the noise in the raw beat note. The scheme uses a mixer as a gating device, introduces an additional optical path to generate a gating signal, and uses a tunable optical delay line to align the optical path. An alternative gated scheme using an ultrahigh-speed track-and-hold amplifier has been proposed for optical frequency measurement [7]. It uses the front-end transistor of the THA chip as a gating

*Corresponding author: shenqi@ustc.edu.cn

†Corresponding author: skliao@ustc.edu.cn

device, while the subsequent integration hold circuit does not contribute to the increase of the final SNR theoretically. These ultrahigh-speed THA chips are usually limited in their selection and relatively expensive.

In this paper, we analyze the SNR model of the beat note and discuss the effects of gating delay and noise on gated-detection-scheme performance. Maximizing the cw-laser power involved in the heterodyne beat can help achieve lower frequency-comb detection power, while bringing additional optical intensity noise. Through an external balun, we build a simple high-speed balanced detector to suppress this optical common-mode noise. Combined with an easy-to-fabricate, low-noise, high-speed generator circuit, which receives a phase-adjustable sinusoidal reference to generate a high-speed gating signal, we realize the optimal gating detection of the beat note. This scheme demonstrates consistent performance improvement over a wide range of comb energy levels. Its reliability is verified in experiments involving locking the frequency comb to an ultrastable laser (USL). Compared with traditional direct-detection schemes, we demonstrate a 20-dB improvement in performance and achieve a beat-note SNR of more than 60 dB within a 300-kHz resolution bandwidth.

II. SNR MODEL

A. Case of balanced detection

In this section, we discuss the direct-detection method with a balanced detector. It is assumed that the spectral shape of the comb after optical bandpass filtering is rectangular, and thus the instantaneous electric field of the cw laser and the frequency comb can be simplified as follows:

$$E_{\text{cw}}(t) = \sqrt{P_{\text{cw}}} e^{i2\pi f_{\text{cw}} t}, \quad (1)$$

$$E_{\text{comb}}(t) = \sum_{n=0}^{N-1} \sqrt{P_{\text{comb},n}} e^{i2\pi(f_0+nf_r)t}, \quad (2)$$

where f_{cw} is the carrier frequency of the cw laser and f_0 is the first tooth of the total N comb teeth within the spectral range of the comb, which has repetition frequency f_r . The average power of the cw laser is denoted by P_{cw} , while $P_{\text{comb},n}$ represents the average power of a single comb tooth of the frequency comb.

The detected beat note between the frequency comb and the cw laser can be expressed as follows:

$$V_{\text{beat}}(t) = 2R(\lambda) \text{Im} \left(\sum_{n=-N_0}^{N_0} \sqrt{P_{\text{cw}} P_{\text{comb},n}} e^{i2\pi(f_{\text{beat}}+nf_r)t} \right), \quad (3)$$

where f_{beat} is the frequency difference between the cw line and comb teeth adjacent to it, N_0 is the number of comb teeth detected by the detector, with $N_0 \sim B_{\text{pd}}/f_r$, B_{pd} is the

bandwidth of the detector, and $R(\lambda)$ is the responsivity of the photodetector (PD).

Here, the noise introduced in the detection process is considered to be mainly from detector noise σ_{PD} , shot noise σ_{SN} , and cw-laser intensity noise σ_{RIN} , which we assume to be independent and uncorrelated white noise [4,14]:

$$\sigma_{n,\text{beat}}^2 = \sigma_{\text{SN}}^2 + \sigma_{\text{PD}}^2 + \sigma_{\text{RIN}}^2, \quad (4)$$

$$\sigma_{\text{SN}} = \sqrt{2qP_{\text{cw}}R(\lambda) \times B_{\text{res}}}, \quad (5)$$

$$\sigma_{\text{PD}} = N_{\text{nep}} \sqrt{B_{\text{res}}} R(\lambda), \quad (6)$$

$$\sigma_{\text{RIN}} = \sqrt{N_{\text{rin,cw}}(B_{\text{res}})} P_{\text{cw}} R(\lambda), \quad (7)$$

where q represents the charge of an electron, B_{res} is the resolution bandwidth of the spectrum analyzer, N_{nep} is the input noise-equivalent power (N_{nep}) of the photodetector, and $N_{\text{rin,cw}}$ is the relative intensity noise (N_{rin}) of the cw laser (the N_{rin} from the comb is ignored here, our assuming that $P_{\text{cw}} \gg P_{\text{comb},n}$). When balanced detection is used, the N_{rin} from the cw laser can be suppressed. Then, we can calculate the SNR of the beat-note signal obtained by direct detection as follows:

$$\text{SNR}_{\text{beat}} = \frac{2R(\lambda)P_{\text{cw}}P_{\text{comb},n}}{[2qP_{\text{cw}} + N_{\text{nep}}^2 R(\lambda)]B_{\text{res}}}. \quad (8)$$

Under the condition of a fixed resolution bandwidth, the main ways to increase the SNR of the beat-note signal include increasing the effective single-mode power of the comb teeth, increasing the cw power, reducing the N_{nep} of the detector, and selecting a photodetector with higher responsivity. However, these methods all have certain limitations and are limited by shot noise [15,16].

B. Case of gated detection

According to Eq. (3), there are high-order coherent harmonics with interval f_r in the spectrum of the beat note. However, only the low-frequency part ($f < f_r/2$) of the beat note is used. By introducing an appropriate local gating signal $V_{\text{LO},\Delta\tau}$, one can superimpose the higher-order harmonic components contained in the original beat note in the low-frequency region through the mixing down-conversion process, which helps to increase the energy-utilization efficiency of the frequency comb.

$$V_{\text{LO},\Delta\tau}(t) = \sum_{m=-M_0}^{M_0} A_{\text{LO},m} e^{i2\pi m f_r(t-\Delta\tau)}, \quad (9)$$

where M_0 represents the number of harmonics in the gating signal, and it should be roughly equivalent to the number of comb teeth N_0 observable by the photodetector to fully exploit the high-order components of the beat note. We define any pulse-overlap moment between the raw beat and

the gating signal in the time domain as the reference plane, and there is a time delay $\Delta\tau$ between the local gating signal and the beat note. We also denote the average amplitude of the harmonic energy of the local gating signal as $A_{LO,m}$.

Then we mix the original beat note V_{beat} with the gating signal $V_{LO,\Delta\tau}$, and output the intermediate-frequency (IF) signal, $V_{IF,\Delta\tau}$, through a low-pass filter with cutoff frequency $f_r/2$:

$$V_{IF,\Delta\tau}(t) = 2R(\lambda)\sqrt{P_{cw}P_{comb,n}}A_{LO,m} \sin(2\pi f_{beat}) \times \sum_{n=-N_0}^{N_0} e^{i2\pi n f_r \Delta\tau}. \quad (10)$$

If we make $\Delta\tau = 0$ and compare it with Eq. (3), it can be seen that the signal here is obtained by duplicating the original signal approximately $2N_0$ times and then amplifying it with the gating signal. The noise terms in Eq. (4) go through a similar process, but they are phase uncorrelated and superimposed as energy signals [13]. It is worth noting that the noise of the local-oscillator (LO) signal, σ_{LO} , is also sampled by the beat-note pulse, and eventually contributes to the overall output noise. We can obtain the SNR of the LO gating signal as $SNR_{LO} = 2A_{LO}^2/\sigma_{LO}^2$.

Then we can calculate the SNR increase of the gated-detection scheme compared with the balanced detection described in Eq. (8) as follows:

$$SNR_{inc} = 2N_0\alpha_\tau^2 \frac{1}{SNR_{beat}/SNR_{LO} + 1}, \quad (11)$$

$$\alpha_\tau = \frac{1}{2N_0} \sum_{n=-N_0}^{N_0} e^{i2\pi n f_r \Delta\tau}, \quad (12)$$

where α_τ describes the effect of the relative delay between the gating signal and the original beat note on the SNR. Under the condition of delay alignment and good gating SNR, we can simplify the above equation to $SNR_{inc} = 2B_{PD}/f_r$.

III. EXPERIMENTAL SETUP

To verify the previous theoretical model, we constructed an experimental setup as shown in Fig. 1. The optical comb system depicted in Fig. 1(a) operates at a repetition frequency of 200 MHz. After dense-wavelength-division-multiplexing (DWDM) filtering, the output spectral width is 0.6 nm (3-dB bandwidth), with the center wavelength being 1550 nm. The output of the USL, operating at a wavelength of 1550 nm, is combined with the output from the comb with the use of a 50:50 beam splitter (BS). The resulting beat-note signal is then captured by the balanced detector. This beat-note signal can be sent to

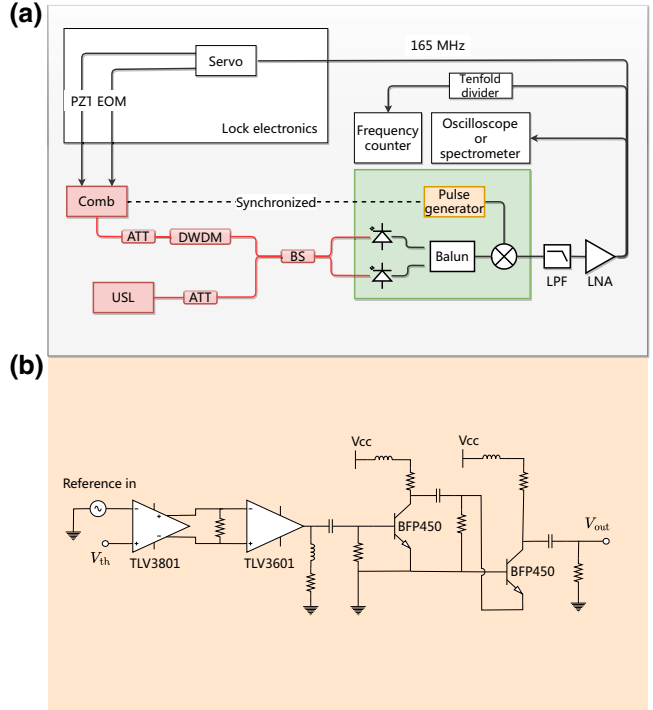


FIG. 1. (a) Simplified scheme for the frequency comb and USL beat-note locking. (b) Pulse generator. ATT, variable attenuator; EOM, electro-optic modulator; LPF, low-pass filter; PZT, piezoelectric transducer.

an external spectrometer and oscilloscope for monitoring purposes. Alternatively, it can be sent to locked electronics to enable referencing of the comb to the USL. In Fig. 1(a), the green-box region represents a device that replaces the single PD originally used to detect the beat note between the frequency comb and the USL. The balanced detector is used to detect the beat-note signal, which is then sent to the signal side of the mixer. The pulse generator [17,18], synchronized to the comb, generates the LO signal required for the mixer operation. The mixer (Mini-Circuits SYM-63LH+) combines the LO and beat-note signals to produce an IF signal, which is further processed by filtering and amplification to obtain the desired beat note. Balanced detection is achieved by our externally combining two 2-GHz photodetectors (Femto HSPR-X-I-2G-IN) using a balun.

A simplified schematic of the pulse generator is shown in Fig. 1(b): the input sine reference signal is shaped by two comparators and a differentiating circuit, triggering the avalanche transistor to generate an avalanche pulse signal. The repetition frequency of the avalanche pulse matches the frequency of the input sinusoidal reference signal, which can be detected directly by a photodetector from the comb, as we do here, or it can be provided by a signal generator whose internal clock is locked to the same signal referencing the comb [7]. To adjust the

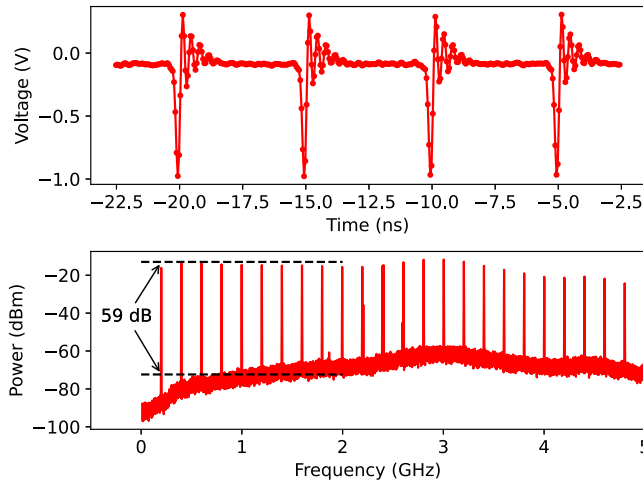


FIG. 2. Time-domain and frequency-domain characteristics of the signal output from the pulse generator.

relative delay of the output narrowband pulse signal, we used a phase shifter (Mini-Circuits SPHSA-251+) to adjust the phase of the reference input through an external dc power supply, and a typical 360° phase shifter can achieve full-cycle (10-ns) delay adjustment. TLV3801 and TLV3601 comparators manufactured by Texas Instruments are used in this setup. These comparators are capable of supporting an input toggle frequency exceeding 200 MHz and exhibit minimal propagation-delay skew, typically just a few picoseconds. To increase both the bandwidth and the amplitude of the pulse, a two-stage triggering structure is used.

The typical time-domain and frequency-domain characteristics of the final output pulse signal are shown in Fig. 2. Three main characteristics of the generated gating signal need to be mentioned here: first, the signal amplitude must fulfill the driving power requirements of the mixer, which necessitates a minimum of 10 dBm or 0.71 V, as illustrated by the red curve; second, the signal bandwidth should be similar to that of the raw beat note to ensure the effective use of the information within the bandwidth of the raw beat, which in this case means it should be at least greater than 2 GHz, as shown by the blue curve; third, the blue curve shows an average SNR of more than 59 dB in the dc 2-GHz range. Generally, a beat-note SNR greater than 30 dB measured with a 300-kHz resolution bandwidth between the frequency comb and the USL is sufficient to meet the basic locking and counting requirements [12], which means that the noise in the local gating signal does not cause significant deterioration of the raw beat note, as described in Eq. (11).

To assess the performance of the current system, we conducted tests on the SNR of the beat note using different frequency-comb powers and USL powers. The theoretically predicted values based on the analysis in Sec. II

are provided. The theoretical calculations used parameters such as the detector's N_{nep} and PD responsivity data from the manufacturer's manual, while the N_{rin} data of our USL were obtained through our fitting experimental data. Additionally, we assume a relative gate delay $\Delta\tau = 0$ in Eq. (12), corresponding to the situation where the photodetector achieves maximum signal-to-noise ratio in practical gated experiments.

We fixed the USL power at 2.2 mW at the BS input port of the USL and recorded the changes in beat-note SNR as the power of the frequency comb was varied from 10 nW to 6 μ W. As shown in Fig. 3(a), compared with the traditional direct-detection method with a single photodetector [trace (i)], balanced detection provides a surprising 10-dB increase in the SNR, shown as trace (ii). The increase of the SNR through balanced detection primarily derives from two aspects. Firstly, balanced detection enables the full utilization of the optical intensity from the BS output, equivalent to twice the optical comb power input of single PD detection. Secondly, effective suppression of N_{rin} from the cw source is achieved, especially in scenarios with strong cw signals. This effect is notably demonstrated by the comparison test results in Fig. 3(b), traces (i) and (ii). Through combination of balanced detection with the gated-detection method, an even greater SNR increase of up to 20 dB for the beat note can be achieved. This results in a more-than-10-dB SNR increase being achievable in the shot-noise-limited direct-detection scheme with a single photodetector, as demonstrated in Fig. 3(a), traces (iii) and (iv). It should be noted that there is a deterioration of approximately 2 dB between the actual measured value and the theoretically calculated value shown in Fig. 3(a), trace (iii-1), calculated through Eqs. (8) and (11). The degradation of the SNR here comes mainly from two aspects: the electrical attenuation used to avoid saturation amplifies the noise from the low-noise amplifier (LNA) (Mini-Circuits PHA-13LN+), and the intensity modulation at around 80.25 and 160.5 MHz from the USL's internal acousto-optic modulator, under high-power conditions adds phase noise in the mixing process. From Fig. 3(c), it can be seen that the raw SNR of direct detection differs from the theoretical calculation by 0.8 dB due to the presence of attenuation and the LNA. The intensity modulation near 160.5 MHz from the USL system is not entirely suppressed by balanced detection. During the mixing process with the 200-MHz gating fundamental, a 39.5-MHz spurious signal is generated. This signal closely approaches our beat note, raising its noise floor. Therefore, we removed the electrical attenuation at the PD output and reduced the power of the USL to 430 μ W. To demonstrate the noise-suppression effect of balanced detection, we chose the beat frequency near the weaker 80-MHz interference. The final test results are shown in Fig. 3(d): it can be seen that the noise sidebands at 80 MHz are effectively suppressed, and the noise floor on both sides of the beat-frequency signal tends to

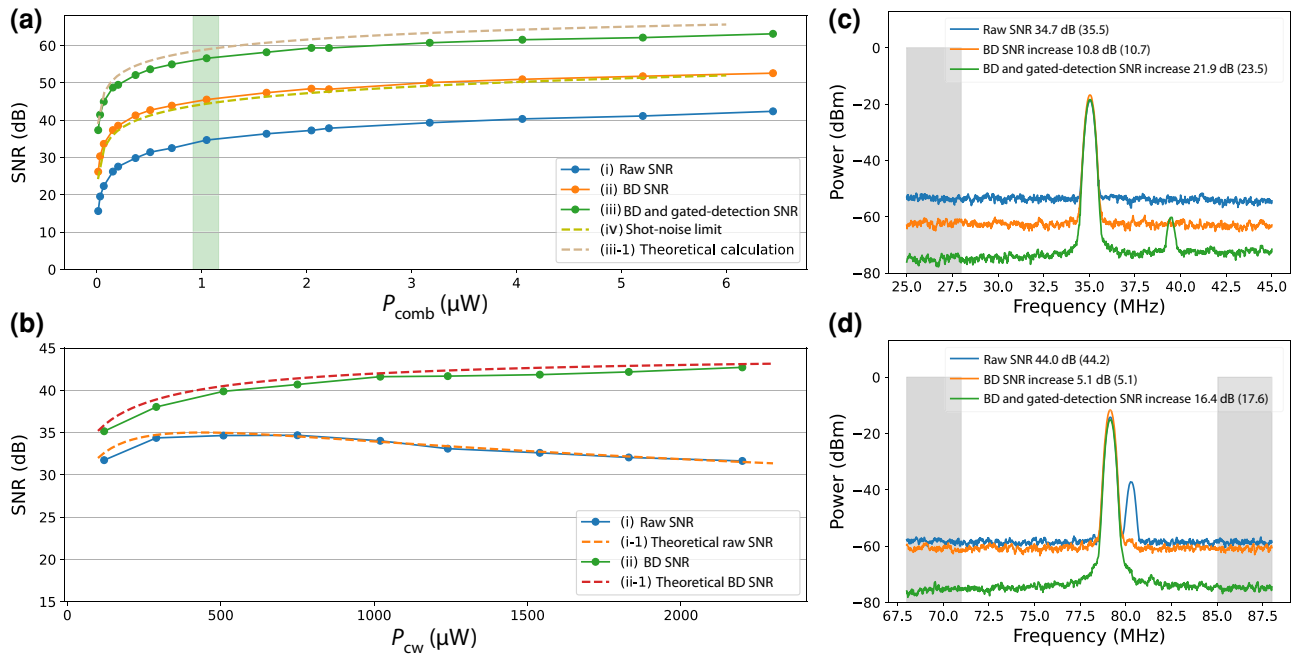


FIG. 3. (a) Comparison of the beat-note SNR with different comb powers for a fixed USL power of 2.2 mW. (b) Beat-note SNR with different USL powers for a fixed comb power of 513 nW. (c) Frequency-domain comparison of beat-note signals obtained from different detection schemes (the resolution bandwidth of the spectrometer is set to 300 kHz), corresponding to the green region in (a). The legend shows the SNR of the original direct detection and the SNR increase of the balanced-detection (BD) and gated-detection schemes based on it. The values in parentheses are the theoretically calculated values. (d) Frequency-domain comparison of beat signals obtained from different detection schemes, with comb power set to 4 μW and USL power set to 430 μW . The gray region here is selected for noise-floor calculation, used to calculate the SNR in this case. The intensity modulation at 160.50 and 80.25 MHz from within the USL system contributes indirectly and directly to the spurious sidebands observed in (c),(d), respectively.

be symmetrical. At the same time, the measured SNR is controlled within a difference of approximately 1.2 dB compared with the theoretical calculation.

Figure 4 also shows the impact of the relative delay between the gating signal and the raw beat-note signal on final SNR increase, indicating that controlling delay differences within tens of picoseconds is necessary (± 66 -ps offset corresponds to 1-dB performance degradation). Here the dashed blue line is calculated according to Eq. (12) and matches the experimental data of the dotted red line.

In the current beat-note-detection scheme, optical balanced detection provides suppression of optical intensity noise and spurious signal, while gated detection achieves high-signal-to-noise-ratio detection at low power levels of the beat-note signal. This contributes to achieving reliable and stable optical locking detection. To demonstrate this, we applied the current measurement system in optical-comb-locking applications and compared it with traditional direct-detection schemes under the same testing conditions. As shown in Fig. 1, the obtained beat note of the comb and the USL is low-pass filtered and amplified by an external low-noise amplification module. This amplified signal is then sent to the comb-lock electronics system to establish a reference between the comb and the USL. In lock electronics, the beat note undergoes a

tenfold division and is subsequently directed to a frequency counter (K+K FXE phase and frequency meter) for frequency measurement. The frequency divider is

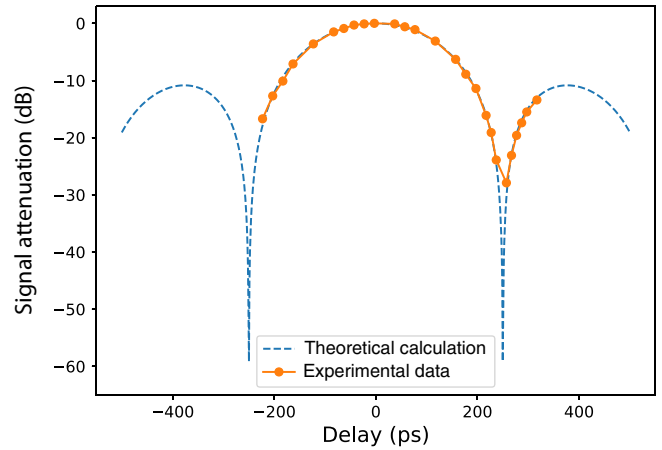


FIG. 4. Relationship between the amplitude of the filtered beat note and the relative-delay variation between the raw beat-frequency signal and the gating pulse. To streamline the calibration process, the delay measurement here used a tunable optical delay line with directly readable delay values, offering a delay accuracy of 1 ps.

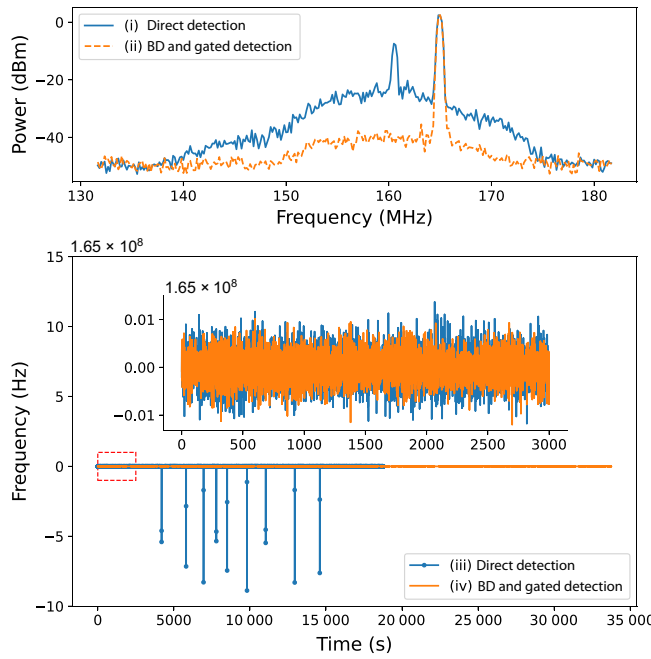


FIG. 5. Top: Beat-note signal of the comb and USL filtered through a 10-MHz-bandwidth bandpass filter. Bottom: Variation of the beat-note-signal frequency over time. Blue curve, direct-detection scheme; orange curve, gated detection combined with balanced detection (BD) scheme.

introduced to accommodate the detection-bandwidth limitation of the counter. Our counter is configured in phase-averaging mode, with a measurement interval set to 1 s. Apart from the beat-note-detection device and inconsistency of measurement time (not simultaneous measurements), the optical link, optical intensity, and frequency-measurement equipment all remained consistent. To minimize environmental disturbances, such as platform vibrations from personnel movement, which could introduce differences in measurement conditions, our frequency-locking measurements were conducted during the night. This is also the reason for the measurement duration being around several hours.

Because of the 80.25-MHz-modulation interference caused by the acousto-optic modulator in the USL system, as well as its second harmonic at 160.5 MHz, the output laser power typically exhibits strong modulation when set to high levels. This results in a corresponding spurious signal in the detected beat-note signal. Hence, the original directly detected 165-MHz beat note for comb locking, despite having an SNR close to 30 dB, exhibits a high probability of phase slip as shown by traces (i) and (iii) in Fig. 5. However, under the same test conditions, with the optical comb output power set to 4 μ W and the USL power at 36 μ W, our approach achieves suppression of this spurious signal and optimization of the SNR. Interference suppression comes mainly from two aspects. Firstly,

balanced detection provides common-mode suppression of interference. Secondly, the energy of interference signals is dispersed into harmonics during the gating mixing process, leading to subsequent suppression. Ultimately, the beat-note signal remains free from phase slip for more than 9 h during observation, indicating the reliability and stability of the detection scheme. This result is illustrated in traces (ii) and (iv) in Fig. 5. It is worth noting that the current measurement results are “in-loop” values, meaning that the signals measured are simultaneously used for phase locking of the optical comb. These signals are insensitive to system noise.

For frequency-measurement-related applications, we are concerned about whether the current pulse generator introduces additional measurement errors. Therefore, it is necessary to compare the frequency measurements of the current scheme with those of traditional single-detector setups. We conducted “out-loop” comparisons between the current detection scheme and traditional single-detector frequency measurements, as shown in Fig. 6: For the comb locked to the 1550-nm USL, its output interfered with the USL output after passing through a DWDM filter (with a linewidth of 0.6 nm). The interference output was split by a 50:50 BS and fed simultaneously to the gating device and a single PD. The beat-note signals from both outputs were monitored simultaneously by two channels of the same frequency counter (K+K FXE phase and frequency meter). The frequency counter operated in phase-averaging mode with a measurement interval of 1 s. It is worth noting that throughout the entire measurement process, the laboratory temperature was maintained at $23 \pm 1^\circ\text{C}$ by the air-conditioning system, and we did not use any other thermal control measures.

Additionally, the same models of bandpass filters and LNAs were used in the back end of both measurement channels. The output signal amplitudes were comparable, with the gated-detection output signal externally connected to a 1-dB attenuator. Since both detection devices share the same optical path, we consider interference in the optical path to be common-mode noise. Therefore, we assume that the differences in frequency measurement primarily originate from the measurement devices themselves.

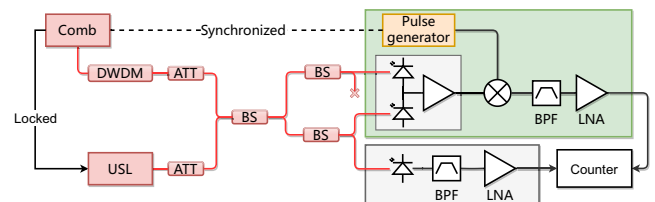


FIG. 6. Experimental setup for comparing the frequency-measurement differences between the traditional single-detector scheme and the gated-detection scheme based on the pulse-generator circuit. ATT, variable attenuator; BPF, bandpass filter.

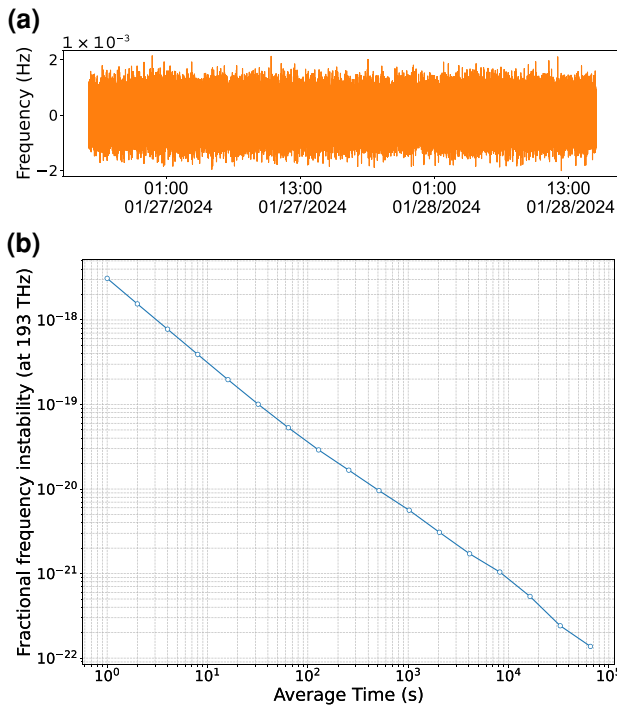


FIG. 7. (a) Variation of measured frequency difference between the single detector and the gated detection over time. (b) Allan variance of the frequency difference between the two detection channels.

Figure 7 depicts the continuous 45-h measurement results, obtained by our subtracting the frequency-measurement data from the two channels of the frequency counter. Figure 7(a) shows the variation of the measured frequency difference between the single detector and the gated detection over time. We computed the average of the entire trajectory, resulting in a frequency difference of approximately 1.2×10^{-8} Hz. Relative to the center frequency of the USL at 193 THz, the measured relative differential ratio is controlled at the level of 6×10^{-23} . Figure 7(b) displays the overlapping Allan deviation curve of the frequency difference. We can observe that its fractional frequency stability reaches 3.1×10^{-18} at 1 s, averaging down to 1.3×10^{-22} , indicating the consistency of the current detection scheme with the original single-detector scheme.

IV. CONCLUSIONS

We show a scheme to optimize the SNR of the beat note between a frequency comb and a cw laser, which achieves an SNR increase of up to 20 dB for beat signals based on an optimized gated detection combined with balanced detection. A wideband-pulse-generator circuit supporting 200-MHz repetition frequency is designed to gate out the noise of the raw beat note. With the current scheme, we achieve an SNR of more than

60 dB at a resolution bandwidth of 300 kHz, without the need to introduce additional optical paths or delay lines. By simply increasing the detection bandwidth of the PD, we can achieve greater SNR increase. The locking experiment demonstrates that the current experimental scheme can provide reliable locking even under adverse conditions such as external interference or low power. This is beneficial for the application of the optical-frequency-comb system under a wider range of measurement conditions. The experimental components are easily accessible or producible and can be conveniently integrated into detection circuits for optical locking or frequency measurements.

ACKNOWLEDGMENTS

This work was supported by the National Key Research and Development Program of China (Grants No. 2020YFA0309800 and No. 2020YFC2200103), the Strategic Priority Research Program of the Chinese Academy of Sciences (Grant No. XDB35030000), the National Natural Science Foundation of China (Grants No. T2125010 and No. 61825505), the Anhui Initiative in Quantum Information Technologies (Grant No. AHY010100), the Key R&D Plan of Shandong Province (Grants No. 2020CXGC010105 and No. 2021ZDPT01), and the Innovation Program for Quantum Science and Technology (Grants No. 2021ZD0300100 and No. 2021ZD0300105). Q.S. is supported by the Youth Innovation Promotion Association of the Chinese Academy of Sciences (Grant No. 2021457).

- [1] L. A. M. Johnson, P. Gill, and H. S. Margolis, Evaluating the performance of the NPL femtosecond frequency combs: Agreement at the 10^{-21} level, *Metrologia* **52**, 62 (2015).
- [2] F. R. Giorgetta, W. C. Swann, L. C. Sinclair, E. Baumann, I. Coddington, and N. R. Newbury, Optical two-way time and frequency transfer over free space, *Nat. Photonics* **7**, 434 (2013).
- [3] Q. Shen, *et al.*, Free-space dissemination of time and frequency with 10^{-19} instability over 113 km, *Nature* **610**, 661 (2022).
- [4] N. R. Newbury, I. Coddington, and W. Swann, Sensitivity of coherent dual-comb spectroscopy, *Opt. Express* **18**, 7929 (2010).
- [5] T. Fortier and E. Baumann, 20 years of developments in optical frequency comb technology and applications, *Commun. Phys.* **2**, 153 (2019).
- [6] L. C. Sinclair, J.-D. Deschênes, L. Sonderhouse, W. C. Swann, I. H. Khader, E. Baumann, N. R. Newbury, and I. Coddington, Invited article: A compact optically coherent fiber frequency comb, *Rev. Sci. Instrum.* **86**, 081301 (2015).
- [7] M. Risaro, P. Savio, M. Pizzocaro, F. Levi, D. Calonico, and C. Clivati, Improving the resolution of comb-based

- frequency measurements using a track-and-hold amplifier, *Phys. Rev. Appl.* **18**, 064010 (2022).
- [8] J.-D. Deschênes and J. Genest, Chirped pulse heterodyne for optimal beatnote detection between a frequency comb and a continuous wave laser, *Opt. Express* **23**, 9295 (2015).
- [9] E. Baumann, F. R. Giorgetta, J. W. Nicholson, W. C. Swann, I. Coddington, and N. R. Newbury, High-performance, vibration-immune, fiber-laser frequency comb, *Opt. Lett.* **34**, 638 (2009).
- [10] Q. Shen, J.-Y. Guan, T. Zeng, Q.-M. Lu, L. Huang, Y. Cao, J.-P. Chen, T.-Q. Tao, J.-C. Wu, L. Hou, S.-K. Liao, J.-G. Ren, J. Yin, J.-J. Jia, H.-F. Jiang, C.-Z. Peng, Q. Zhang, and J.-W. Pan, Experimental simulation of time and frequency transfer via an optical satellite–ground link at 10^{-18} instability, *Optica* **8**, 471 (2021).
- [11] J. Lee, K. Lee, Y.-S. Jang, H. Jang, S. Han, S.-H. Lee, K.-I. Kang, C.-W. Lim, Y.-J. Kim, and S.-W. Kim, Testing of a femtosecond pulse laser in outer space, *Sci. Rep.* **4**, 5134 (2014).
- [12] H. Leopardi, J. Davila-Rodriguez, F. Quinlan, J. Olson, J. A. Sherman, S. A. Diddams, and T. M. Fortier, Single-branch Er:fiber frequency comb for precision optical metrology with 10^{-18} fractional instability, *Optica* **4**, 879 (2017).
- [13] J.-D. Deschênes and J. Genest, Heterodyne beats between a continuous-wave laser and a frequency comb beyond the shot-noise limit of a single comb mode, *Phys. Rev. A* **87**, 023802 (2013).
- [14] S. B. Alexander, *Optical Communication Receiver Design*, SPIE Tutorial Texts in Optical Engineering, Vol. TT 22 (SPIE Optical Engineering Press/Institution of Electrical Engineers, Bellingham, USA/London, UK, 1997).
- [15] K. Imai, B. Widjyatmoko, M. Kourogi, and M. Ohtsu, 12-THz frequency difference measurements and noise analysis of an optical frequency comb in optical fibers, *IEEE J. Quantum Electron.* **35**, 559 (1999).
- [16] H. Bergeron, J.-D. Deschênes, and J. Genest, Improving the signal-to-noise ratio of the beatnote between a frequency comb and a tunable laser using a dynamically tracking optical filter, *Opt. Lett.* **41**, 4253 (2016).
- [17] H. Zhang, X. Liu, N. Li, and T. A. Gulliver, in *Proceedings of 2011 IEEE Pacific Rim Conference on Communications, Computers and Signal Processing* (IEEE, Victoria, BC, Canada, 2011), p. 691.
- [18] R. Feghhi, R. Winter, and K. Rambabu, A high-performance UWB Gaussian pulse generator: analysis and design, *IEEE Trans. Microw. Theory Tech.* **70**, 3257 (2022).